Regularity-Aware Stochastic MGDA with Adaptive Conflict-Avoidant Update Direction Control

Chentong Huang, Lisha Chen
Dept. of Electrical and Computer Engineering, University of Rochester, Rochester, NY 14627
E-mails: chuang80@ur.rochester.edu, lisha.chen@rochester.edu

***Abstract*—Multi-objective learning (MOL) aims to optimize multiple objectives simultaneously. The multi-gradient descent algorithm (MGDA) is a workhorse that iteratively updates along a common descent or conflict-avoidant (CA) direction across objectives. In stochastic settings, however, the vanilla stochastic MGDA method, SMG [1], lacks a fast convergence rate because mini-batch sampling introduces noise in the gradients. This causes bias in the update direction, which is controlled by the CA direction continuity. In this paper, we show that the CA direction is $1/2$-Hölder continuous with respect to the Jacobian matrix, and the exponent $1/2$ cannot be improved in the worst case. This leads to a suboptimal convergence rate for vanilla stochastic MGDA in prior works. Nevertheless, under additional regularity conditions, we show this can be improved to Lipschitz continuity. Based on this insight, we propose a stochastic multi-objective regularity-aware (MoRe) method that exploits the Lipschitz continuity of the CA direction when the subproblem is regular, and switches to a fixed scalarization weight otherwise. Intuitively, the proposed algorithm employs CA direction update when the gradient conflict is large, and linear scalarization update otherwise. Theoretically, our method improves the convergence rate of SMG [1], [2] in the nonconvex setting from $\widetilde{\mathcal{O}}(T^{-1/4})$ to $\widetilde{\mathcal{O}}(T^{-1/2})$, where $\widetilde{\mathcal{O}}(\cdot)$ hides logarithmic factors. Meanwhile, we also establish the per-iterate conflict-avoidance guarantees. Empirically, experiments demonstrate its effectiveness in multi-task performance and verify convergence behavior consistent with the established theoretical rate.**

***Index Terms*—multi-objective optimization, stochastic optimization, conflict avoidance, multi-task learning.**

I. INTRODUCTION

Multi-objective learning (MOL) has emerged as an important paradigm in modern machine learning. Representative applications include multi-task learning [3], meta learning [4], [5], and learning under multiple constraints [6].

In this work, we consider the empirical MOL problem defined on a training sample sequence $S = (z_1, \dots, z_n) \in \mathcal{Z}^n$. Let $[M] \coloneqq \{1, \dots, M\}$, where $M \geq 2$. For each objective $m \in [M]$, let $f_{z,m}(x)$ denote the m-th objective function evaluated at model $x \in \mathbb{R}^p$ on a data point z, and define its empirical counterpart by $f_{S,m}(x) \coloneqq n^{-1} \sum_{i=1}^{n} f_{z_i,m}(x)$. The empirical MOL problem is formulated as the optimization of the vector-valued objective:

$$\min_{x \in \mathbb{R}^p} F_S(x) \coloneqq \big(f_{S,1}(x), \dots, f_{S,M}(x)\big)^\top. \tag{1}$$

Unlike single-objective learning, MOL seeks a Pareto optimal or Pareto stationary solution rather than the minimizer of a scalar loss. One of the central challenges is that the gradients of different objectives may conflict: a descent direction for one objective may increase another. A widely used strategy by many methods [2], [7], [8] is to dynamically combine objective gradients to obtain a conflict-avoidant (CA) direction. Among the methods, a representative approach is MGDA [7], [9], [10], which computes a minimum-norm convex combination of objective gradients and has motivated many variants for MOL [2], [8], [11]. While the deterministic MGDA variants are relatively well studied, full-batch gradients are typically too expensive to compute at every iteration in practice, especially for large machine learning models. This has motivated stochastic variants of MGDA, such as the stochastic multi-gradient (SMG) method [1], which replaces the full-batch gradient matrix with stochastic gradient estimates computed from mini-batches.

However, directly extending the convergence analysis of MGDA to the stochastic setting is nontrivial. Since the CA direction is a nonlinear function of the gradient matrix, replacing the full-batch gradient matrix with a mini-batch estimate can introduce direction bias: the mini-batch CA direction may not be an unbiased or stable approximation of the full-batch CA direction. This sensitivity can be characterized by α-Hölder continuity of the direction mapping: for gradient matrices $Q_1, Q_2 \in \mathbb{R}^{p \times M}$,

$$\|d_{Q_1} - d_{Q_2}\| \leq \ell_{\mathrm{H}} \|Q_1 - Q_2\|^\alpha, \tag{2}$$

where $\ell_{\mathrm{H}} > 0$ is the Hölder constant, $\alpha \in (0, 1]$, and $\alpha = 1$ corresponds to Lipschitz continuity. Despite its direct relevance to the stability and convergence of stochastic MGDA methods, exploration of this question remains limited in the existing literature. Specifically, [12] proved that the CA direction is $1/2$-Hölder continuous with respect to the model variable x, and that the exponent $1/2$ is sharp. In addition, [2] showed a corresponding $1/2$-Hölder continuity result with respect to the stochastic gradient matrix. This motivates us to investigate when stronger regularity can hold, and to exploit such properties in the design of stochastic algorithms with improved convergence guarantees while preserving conflict-avoidance behavior.

A. *Related work*

Deterministic gradient-based MOL. A major line of work in MOL seeks a common update direction for all objectives using gradient information. A foundational method in this direction is MGDA [7], [9], [10], which dynamically combines gradients to obtain a common descent direction. Beyond MGDA, several gradient-aggregation methods have been proposed to mitigate conflicts among objectives. For example, PCGrad [13] projects conflicting task gradients, while CAGrad [8] seeks a conflict-averse aggregated direction. These methods highlight the importance of conflict-aware gradient aggregation in MOL. However, in large-scale learning and modern deep learning applications, full-batch gradients are typically too expensive to compute at every iteration.

Stochastic MOL. Practical MOL algorithms usually require updates based on (mini-batch) stochastic gradients, which has motivated stochastic extensions of MGDA. For instance, SMG [1] extends MGDA to the stochastic setting and provides convergence guarantees. Subsequent works further develop provably convergent stochastic MOL algorithms using different sampling, variance-reduction, and preference-guided mechanisms [2], [11], [14]–[18]. For convergence analysis, a key obstacle lies in controlling update-direction bias and conflict-avoidance error: since the CA direction depends nonlinearly on the gradient matrix, stochastic gradient noise can create CA-direction error. This in turn affects the convergence analysis of the stochastic variants of MGDA, and may lead to suboptimal convergence rates, as discussed in [2], and summarized in Table I.

Continuity of the CA direction map. The continuity of the CA direction mapping is important for stochastic MOL because it controls the CA direction error. Earlier work studied the continuity of the CA direction with respect to the model variable and established a $1/2$-Hölder continuity result [12]. For stochastic MOL, Chen et al. [2] prove a $1/2$-Hölder continuity result with respect to the stochastic gradient matrix. However, these results do not characterize when stronger Lipschitz continuity with respect to the gradient matrix is available, nor do they explore whether it can be exploited to obtain faster stochastic convergence and more stable CA directions. Our work addresses this gap by identifying a nondegenerate Lipschitz regime of the direction map and exploiting it through a regularity-aware stochastic algorithm.

B. Our contributions

Our contributions in this paper are summarized as follows.

Continuity analysis of the CA direction. We provide a fine-grained continuity analysis of the CA direction mapping. Under a nondegeneracy condition in Definition 2, Lemma 1 proves Lipschitz continuity of the CA direction mapping, while Lemma 2 shows that without the nondegeneracy condition, the $1/2$-Hölder continuity on bounded sets is sharp in the worst case.

Improved convergence guarantees. Motivated by the above continuity properties, we develop a Multi-objective Regularity-aware (MoRe) algorithm that leverages the regularity of the CA direction in different regimes. With mini-batch sizes $|Z_t| = \Theta(t+1)$ and step size $\alpha = \Theta(T^{-1/2})$, Theorem 1 gives the nonconvex empirical stationarity rate $\widetilde{\mathcal{O}}(T^{-1/2})$, improving the $\widetilde{\mathcal{O}}(T^{-1/4})$ SMG rate in [2]. Theorem 2 further establishes a per-iterate CA direction distance bound. See Table I for a comparison with existing methods.

Experiments on MTL applications. We compare the proposed method with existing MOL algorithms, and the empirical results demonstrate its practical effectiveness in both model performance and convergence behavior.

TABLE I

COMPARISON WITH PRIOR STOCHASTIC MOL ALGORITHMS IN BATCH SIZE, CONVERGENCE RATE, AND CA DIRECTION DISTANCE. HERE, CONV. AND CA DIST. DENOTE THE CONVERGENCE RATE AND CA DIRECTION DISTANCE, RESPECTIVELY, AND $\widetilde{\mathcal{O}}(\cdot)$ HIDES LOGARITHMIC FACTORS. NOTE THAT THE RESULT OF MODO [2] IS OBTAINED BY OPTIMALLY TUNING THE HYPERPARAMETERS IN THE THEOREMS THEREIN.

Algorithm	Batch size	Conv.	CA Dist.
SMG [1] [2, Thms 7,8]	$\Theta(t+1)$	$\widetilde{\mathcal{O}}(T^{-\frac{1}{4}})$	per-iterate
CR-MOGM [14, Thm 3]	$\Theta(1)$	$\mathcal{O}(T^{-\frac{1}{2}})$	-
MoCo [11, Thm 2]	$\Theta(1)$	$\mathcal{O}(T^{-\frac{1}{10}})$	average
MoDo [2, Thms 3,5]	$\Theta(1)$	$\widetilde{\mathcal{O}}(T^{-\frac{1}{2}})$	average
MoCo+ [18, Thms 1,2]	$\Theta(1)$	$\mathcal{O}(T^{-\frac{2}{3}})$	average
Ours, Thm 1, 2	$\Theta(t+1)$	$\widetilde{\mathcal{O}}(T^{-\frac{1}{2}})$	per-iterate

II. PROBLEM SETUP

In this section, we introduce some basic concepts in MOL problems. We briefly introduce the corresponding population objective F only to state the standard notions of Pareto stationarity and Pareto optimality. Let $F(x) := (f_1(x), \dots, f_M(x))^\top$, where $f_m(x) := \mathbb{E}_z[f_{z,m}(x)]$. Our optimization and convergence analysis focus on the empirical objective F_S defined above. The same definitions apply to the empirical problem after replacing F by F_S.

Definition 1 (Pareto optimal and Pareto stationary points)**.** *A point $x^* \in \mathbb{R}^p$ is called Pareto optimal if there does not exist any $x \in \mathbb{R}^p$ with $x \neq x^*$ such that $f_m(x) \leq f_m(x^*)$ for all $m \in [M]$ and $f_{m'}(x) < f_{m'}(x^*)$ for at least one $m' \in [M]$. It is called weakly Pareto optimal if there does not exist any $x \in \mathbb{R}^p$ such that $f_m(x) < f_m(x^*)$ for all $m \in [M]$. A point $x \in \mathbb{R}^p$ is called Pareto stationary if there exists $\lambda \in \Delta^M$ such that $\nabla F(x)\lambda = 0$, where $\Delta^M := \{\lambda \in \mathbb{R}^M \mid \mathbf{1}^\top \lambda = 1,\ \lambda \geq 0\}$, and $\nabla F(x) := \big(\nabla f_1(x), \nabla f_2(x), \dots, \nabla f_M(x)\big) \in \mathbb{R}^{p \times M}$.*

By definition, a Pareto stationary point admits no common descent direction for all objectives. For smooth objectives, a necessary and sufficient condition for x to be Pareto stationary [19] is $\min_{\lambda \in \Delta^M} \|\nabla F(x)\lambda\| = 0$. Therefore, the quantity $\min_{\lambda \in \Delta^M} \|\nabla F(x)\lambda\|$ can be used as a measure of Pareto stationarity [2], [10], [11]. Accordingly, since our analysis is conducted on the empirical objective F_S, we define the empirical Pareto-stationarity measure

$$R_S(x) := \min_{\lambda \in \Delta^M} \|\nabla F_S(x)\lambda\|^2. \tag{3}$$

A. Multi-gradient descent algorithm (MGDA)

To solve the multi-objective problem, MGDA [10] constructs a common descent direction for all objectives. At each iteration, MGDA seeks a direction $d(x) \in \mathbb{R}^p$ that improves all objectives simultaneously. In particular, one solves

$$d(x) = -\nabla F_S(x)\lambda^*(x) \tag{4}$$

$$\text{s.t.} \quad \lambda^*(x) \in \arg\min_{\lambda \in \Delta^M} \|\nabla F_S(x)\lambda\|^2 . \tag{5}$$

Here, $\lambda^*(x)$ denotes the simplex-constrained weight vector used to combine the objective gradients. The t-th iterate is then updated by

$$x_{t+1} = x_t + \alpha_t d(x_t), \tag{6}$$

where $\alpha_t > 0$ is the step size. The resulting direction $d(x_t)$ is a common descent direction whenever x_t is not Pareto stationary. Moreover, MGDA terminates when $\nabla F_S(x_t)\lambda^*(x_t) = 0$, in which case x_t is a Pareto stationary point.

B. Stochastic multi-objective gradient (SMG) method

A natural stochastic counterpart of MGDA is the SMG method [1], which replaces the full-batch gradients by stochastic gradient estimates computed from sampled data. Specifically, let $Z = (\zeta_1, \ldots, \zeta_{|Z|})$ denote a mini-batch sampled i.i.d. uniformly from S, equivalently with replacement. Define

$$\nabla F_Z(x) \coloneqq \frac{1}{|Z|}\sum_{r=1}^{|Z|} \nabla F_{\zeta_r}(x), \tag{7}$$

where $F_z(x) = \big(f_{z,1}(x), \ldots, f_{z,M}(x)\big)$ collects the objective values evaluated at sample z. For notational simplicity, let $Q \in \mathbb{R}^{p\times M}$ denote the stochastic gradient matrix $\nabla F_Z(x)$,

$$Q \coloneqq \nabla F_Z(x) = [q_{Z,1}(x), \ldots, q_{Z,M}(x)] \in \mathbb{R}^{p\times M}, \tag{8}$$

where $q_{Z,m}(x) \coloneqq \frac{1}{|Z|}\sum_{r=1}^{|Z|} \nabla f_{\zeta_r,m}(x) \in \mathbb{R}^p$. Define

$$g_Q(\lambda) \coloneqq \|Q\lambda\|^2, \qquad \lambda \in \Delta^M. \tag{9}$$

Then SMG computes the stochastic descent direction as

$$d_Q = -Q\lambda_Q^*, \quad \text{s.t.} \quad \lambda_Q^* \in \arg\min\nolimits_{\lambda\in\Delta^M} g_Q(\lambda), \tag{10}$$

where $d_Q \in \mathbb{R}^p$ denotes the update direction associated with Q, and $\lambda_Q^* \in \Delta^M$ denotes an optimal simplex weight for Q.

To measure how well the update direction tracks the corresponding full-batch CA direction, we further adopt the CA direction distance introduced in [2]. The CA direction distance at the t-th iteration is defined as

$$\mathcal{E}_{\mathrm{ca}}(t) \coloneqq \left\|\mathbb{E}[d_t - d(x_t)]\right\|^2, \quad d(x_t) = -\nabla F_S(x_t)\lambda^*(x_t), \tag{11}$$

where $\lambda^*(x_t) \in \arg\min_{\lambda\in\Delta^M} \|\nabla F_S(x_t)\lambda\|^2$, and d_t is the update direction at the t-th iteration. The expectation in $\mathcal{E}_{\mathrm{ca}}(t)$ is unconditional and is taken over the algorithmic randomness. This quantity measures the discrepancy between the stochastic update direction d_t and the full-batch CA direction $d(x_t)$. It is therefore used to characterize the conflict-avoidance ability of stochastic MOL algorithms.

III. REGULARITY-AWARE STOCHASTIC MGDA

In this section, we first study the continuity properties of the CA direction mapping, identifying the conditions under which it is Lipschitz continuous and the regimes in which only 1/2-Hölder continuity is available. Motivated by these findings, we then develop a stochastic Multi-objective Regularity-aware (MoRe) algorithm and establish its convergence and conflict-avoidance guarantees.

A. Continuity properties of the CA direction mapping

Although the optimizer λ_Q^* of the simplex subproblem (10) may not be unique, the resulting direction $d_Q = -Q\lambda_Q^*$ is unique, since it is the minimum-norm point in the convex hull of $\{q_{Z,1}(x), \ldots, q_{Z,M}(x)\}$. We show that the mapping $Q \mapsto d_Q$ is Lipschitz continuous under a suitable nondegeneracy condition, but in general only $1/2$-Hölder continuous on bounded sets.

Definition 2 (μ-nondegeneracy). *Let $P := I - \frac{1}{M}\mathbf{1}\mathbf{1}^\top$ be the orthogonal projector onto $\mathbf{1}^\perp := \{v \in \mathbb{R}^M : \mathbf{1}^\top v = 0\}$. Let $U \in \mathbb{R}^{M\times(M-1)}$ be any matrix whose columns form an orthonormal basis of $\mathbf{1}^\perp$, so that $U^\top U = I$ and $UU^\top = P$. We say a matrix $Q \in \mathbb{R}^{p\times M}$ is μ-nondegenerate if*

$$\mu_{\min}\big(U^\top Q^\top Q U\big) \geq \mu. \tag{12}$$

Equivalently, $\|Qv\|^2 \geq \mu\|v\|^2$ for every $v \in \mathbf{1}^\perp$.

Definition 2 imposes a uniform positive-curvature condition on the dual subproblem (10) restricted to feasible simplex directions. In particular, $U^\top Q^\top Q U$ is the reduced curvature matrix on the tangent space of the simplex, and the lower bound $\mu_{\min}(U^\top Q^\top Q U) \geq \mu$ rules out degeneracy in this reduced space. Equivalently, the quadratic objective $g_Q(\lambda) = \|Q\lambda\|^2$ is strongly convex on the affine hull of the simplex, i.e., along directions in $\mathbf{1}^\perp$. This reduced strong convexity yields uniqueness of the MGDA weight and allows perturbations of the optimality conditions to be controlled directly, which is the key ingredient used to establish Lipschitz continuity of the CA direction mapping.

Lemma 1 (Lipschitz continuity of d_Q w.r.t. Q). *Suppose $Q_1, Q_2 \in \mathbb{R}^{p\times M}$ satisfy $\|Q_i\|_F \leq B$ and are μ-nondegenerate in the sense of Definition 2; that is, $\mu_{\min}\big(U^\top Q_i^\top Q_i U\big) \geq \mu$, for $i = 1, 2$. Then the mapping $Q \mapsto d_Q$ is Lipschitz continuous. In particular, there exists a constant $\ell_d = 1 + \frac{2B^2}{\mu}$ such that*

$$\|d_{Q_1} - d_{Q_2}\| \leq \ell_d\|Q_1 - Q_2\|. \tag{13}$$

Here $\|\cdot\|$ denotes the spectral norm for matrices. Since $\|A\| \leq \|A\|_F$, the same bound also holds with $\|Q_1 - Q_2\|_F$ on the right-hand side.

Lemma 1 shows that, on any bounded set of matrices satisfying Definition 2, the CA direction depends Lipschitz continuously on the gradient matrix. Consequently, mini-batch noise in Q translates into controlled errors in the update direction d_Q, which is essential for the convergence analysis of stochastic MGDA methods. The proof of Lemma 1 is deferred to Appendix A.

Lemma 2 (Sharpness of the $1/2$-Hölder exponent). *For any $Q, Q' \in \mathbb{R}^{p\times M}$ satisfying $\|Q\|_F \leq B$ and $\|Q'\|_F \leq B$, the mapping $Q \mapsto d_Q$ is $1/2$-Hölder continuous on this bounded set; moreover, without additional assumptions, no Hölder continuity with exponent $\eta > \frac{1}{2}$ holds in general.*

Lemma 2 indicates that the continuity result in Lemma 1 cannot be extended to the general case. Lemma 2 also agrees with the $1/2$-Hölder continuity of the CA direction mapping established in [2], while further showing that the exponent

Algorithm 1 MoRe: Multi-objective Regularity-aware method

input training data $S = (z_1, \ldots, z_n)$, initial model x_0, step sizes $\{\alpha_t\}_{t=0}^{T-1}$, batch sizes $\{|Z_t|\}_{t=0}^{T-1}$, thresholds $\{\mu_t\}_{t=0}^{T-1}$, fallback weight $\lambda_0 \in \Delta^M$, and an orthonormal basis $U \in \mathbb{R}^{M\times(M-1)}$ of $\mathbf{1}^\perp$.
for $t = 0, \ldots, T-1$ **do**
  Sample Z_t i.i.d. uniformly from S
  Compute $Q_t = [q_{Z_t,1}(x_t), \ldots, q_{Z_t,M}(x_t)]$
  if $\mu_{\min}(U^\top Q_t^\top Q_t U) \geq \mu_t$ **then**
    Update λ_t by (14)
  else
    set $\lambda_t = \lambda_0$
  end if
  Update x_{t+1} by (15)
end for
output x_T.

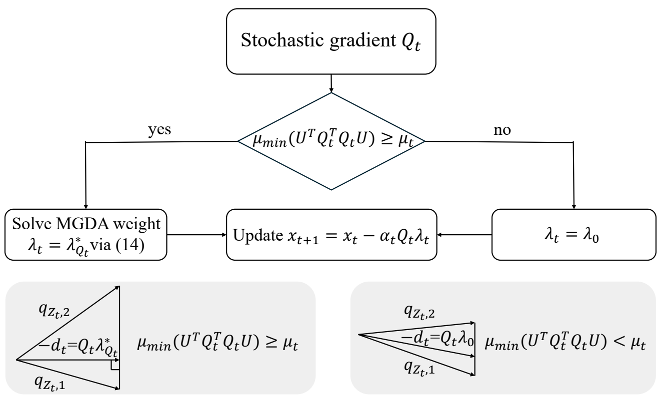

Fig. 1. Flowchart of the proposed MoRe algorithm. The illustrations show the switching rule in the two-objective case, where $\mu_{\min}(U^\top Q_t^\top Q_t U) = \frac{1}{2}\|q_{Z_t,1} - q_{Z_t,2}\|^2$ measures the distance or conflict between the two stochastic gradients. When $\mu_{\min}(U^\top Q_t^\top Q_t U) \geq \mu_t$, the algorithm uses the MGDA conflict-avoidant update direction. Otherwise, the stochastic gradient matrix is treated as nearly degenerate and the algorithm switches to the fixed-weight scalarization direction $d_t = -Q_t\lambda_0$.

$\frac{1}{2}$ is sharp in the worst case. This is analogous to the result in [12], which establishes $1/2$-Hölder continuity of the CA direction with respect to the model variable x and shows that the exponent is optimal. Therefore, stochastic MGDA may behave differently in regular and degenerate regimes: in regular regimes, mini-batch perturbations in Q induce Lipschitz-controlled changes in d_Q, whereas in degenerate regimes, only $1/2$-Hölder control is available. This distinction motivates the adaptive strategy developed in Algorithm 1. The proof of Lemma 2 is deferred to Appendix B.

B. Regularity-aware stochastic MGDA

Building on the continuity results above, we propose a regularity-aware stochastic MGDA method. In particular, Lemma 1 shows that the CA direction is Lipschitz continuous w.r.t. Q under a nondegeneracy condition. Hence, mini-batch noise in Q only induces a proportionally controlled perturbation in the resulting update direction. In contrast, Lemma 2 shows that such Lipschitz stability may fail in degenerate regimes where small stochastic perturbations of Q can lead to much larger changes in the CA direction.

Motivated by this distinction, as shown in Figure 1, Algorithm 1 adaptively switches between the stochastic MGDA weight and a fixed scalarization weight according to the regularity of the stochastic gradient matrix. When the stochastic MGDA subproblem is well-conditioned, the algorithm uses the CA direction to exploit CA gradient aggregation. When the subproblem is degenerate or nearly degenerate, the MGDA weight can be highly sensitive to mini-batch noise; the algorithm therefore uses a fixed scalarization weight λ_0, or static weighting, to avoid amplifying the noise in the optimizer of the simplex subproblem. The fallback weight λ_0 can be chosen as any prescribed simplex vector reflecting a preferred scalarization; for example, in our experiments, we use the uniform choice $\lambda_0 = \frac{1}{M}\mathbf{1}$.

Specifically, at iteration t, a mini-batch Z_t is drawn independently with replacement from the empirical distribution on S. We then form the stochastic gradient matrix $Q_t = \big[q_{Z_t,1}(x_t), \ldots, q_{Z_t,M}(x_t)\big]$, which collects the mini-batch stochastic gradients $q_{Z_t,m}(x_t)$ for $m \in [M]$. When the nondegeneracy condition $\mu_{\min}\big(U^\top Q_t^\top Q_t U\big) \geq \mu_t$ holds, we compute the MGDA weight by solving

$$\lambda_t = \lambda^*_{Q_t} \in \operatorname*{arg\,min}_{\lambda \in \Delta^M} \|Q_t\lambda\|^2. \tag{14}$$

Otherwise, the algorithm falls back to a fixed simplex weight $\lambda_t = \lambda_0 \in \Delta^M$. In both cases, the model is updated by

$$x_{t+1} = x_t - \alpha_t Q_t \lambda_t. \tag{15}$$

That is, the proposed method uses the stochastic CA direction when the nondegeneracy condition holds, and switches to a fixed scalarization rule otherwise. The threshold sequence $\{\mu_t\}_{t\geq 0}$ controls how strict the algorithm is in declaring the stochastic MGDA subproblem to be well-conditioned. We set the threshold schedule $\{\mu_t\}_{t\geq 0}$ so that $0 < \mu_t \leq \bar{\mu}$ for some finite constant $\bar{\mu}$.

This design exploits the continuity of the CA direction in nondegenerate regimes and avoids relying on it in degenerate regimes, where the update direction can be sensitive to mini-batch noise.

C. Theoretical analysis

In this subsection, we provide theoretical guarantees for the proposed MoRe method. We first introduce the assumptions used throughout the analysis, and then establish convergence in terms of the Pareto stationarity measure, together with bounds on the CA direction distance.

Assumption 1 (Finite lower bounds)**.** *For each* $m \in [M]$, $\inf_x f_{S,m}(x) > -\infty$.

Assumption 1 is mild and standard in convergence analysis. It ensures that every fixed scalarization of the empirical objectives is bounded below.

Assumption 2 (Unbiasedness and bounded variance)**.** *Let* $\mathcal{F}_t$ *be the sigma-field generated by all randomness up to the beginning of iteration t, before sampling* Z_t*. Conditional on* $\mathcal{F}_t$, $Z_t = (\zeta_{t,r})_{r=1}^{|Z_t|}$ *is sampled i.i.d. uniformly from S. There exists a constant* $\sigma > 0$*, independent of* t, m*, and* *the algorithmic trajectory, such that for every t and every $m \in [M]$, almost surely,*

$$\mathbb{E}[q_{Z_t,m}(x_t) \mid \mathcal{F}_t] = \nabla f_{S,m}(x_t), \tag{16}$$

$$\mathbb{E}\big[\|q_{Z_t,m}(x_t) - \nabla f_{S,m}(x_t)\|^2 \mid \mathcal{F}_t\big] \le \frac{\sigma^2}{|Z_t|}. \tag{17}$$

Assumption 2 requires the stochastic gradients to be unbiased and to have bounded variance. This is standard in stochastic optimization [1], [11], and will be used to control the stochastic error introduced by mini-batch gradient estimation.

Assumption 3 (Smoothness)**.** *There exists a constant $\ell_{f,1} > 0$ such that, for every $\lambda \in \Delta^M$, the scalarized empirical objective $x \mapsto \lambda^\top F_S(x)$ is $\ell_{f,1}$-smooth on $\mathbb{R}^p$.*

Assumption 4 (Bounded gradients)**.** *There exist finite positive constants ℓ_f and $\ell_F = \sqrt{M}\ell_f$ such that, for every $x \in \mathbb{R}^p$, $z \in \mathcal{Z}$, and $m \in [M]$, $\|\nabla f_{z,m}(x)\| \le \ell_f$. Since $q_{Z,m}(x) = |Z|^{-1}\sum_{r=1}^{|Z|} \nabla f_{\zeta_r,m}(x)$, the triangle inequality gives $\|q_{Z,m}(x)\| \le \ell_f$. Therefore, for every mini-batch Z, every t, and every $\lambda \in \Delta^M$,*

$$\begin{aligned} &\|Q_t\lambda\| \le \ell_f, \quad \|\nabla F_S(x_t)\lambda\| \le \ell_f, \\ &\|Q_t\|_F \le \ell_F, \quad \|\nabla F_S(x_t)\|_F \le \ell_F. \end{aligned} \tag{18}$$

Assumptions 3 and 4 are also standard in gradient-based MOL analysis [2]. Assumption 3 is used to establish the descent property of the scalarized objective, while Assumption 4 controls the magnitudes of both the empirical and stochastic gradients along the optimization trajectory.

Theorem 1. *Suppose Assumptions 1, 2, 3, and 4 hold. Let $\alpha_t = \alpha$ for all t, and let the threshold sequence satisfy $0 < \mu_t \le \bar{\mu}$ for a finite constant $\bar{\mu}$. Then the iterates generated by Algorithm 1 satisfy*

$$\mathbb{E}\Big[\min_{0\le t\le T-1} R_S(x_t)\Big] \le \mathcal{O}\Bigg(\frac{1}{\alpha T} + \alpha + \frac{1}{T}\sum_{t=0}^{T-1}\frac{1}{\sqrt{|Z_t|}} + \frac{1}{T}\sum_{t=0}^{T-1}\frac{1}{\mu_t\sqrt{|Z_t|}} + \frac{1}{T}\sum_{t=0}^{T-1}\frac{1}{|Z_t|\mu_t^{3/2}}\Bigg). \tag{19}$$

Suppose the mini-batch sizes and the constant step size satisfy

$$|Z_t| = \Theta(t+1), \qquad \alpha = \Theta(T^{-1/2}). \tag{20}$$

Under this schedule, the following two consequences hold. If $\mu_t = \Theta(1)$, then

$$\mathbb{E}\Big[\min_{0\le t\le T-1} R_S(x_t)\Big] = \mathcal{O}(T^{-1/2}). \tag{21}$$

If instead $\mu_t = \Theta\Big(\frac{1}{\log(e+t)}\Big)$, then

$$\mathbb{E}\Big[\min_{0\le t\le T-1} R_S(x_t)\Big] = \widetilde{\mathcal{O}}(T^{-1/2}). \tag{22}$$

Theorem 1 shows that the regularity threshold μ_t controls the convergence rate through the continuity of the CA direction mapping. In particular, a uniformly positive threshold gives the exact $\mathcal{O}(T^{-1/2})$ rate, whereas a logarithmically decaying threshold preserves a $\widetilde{\mathcal{O}}(T^{-1/2})$ rate while allowing the CA direction distance to decay. The detailed proof is provided in Appendix C.

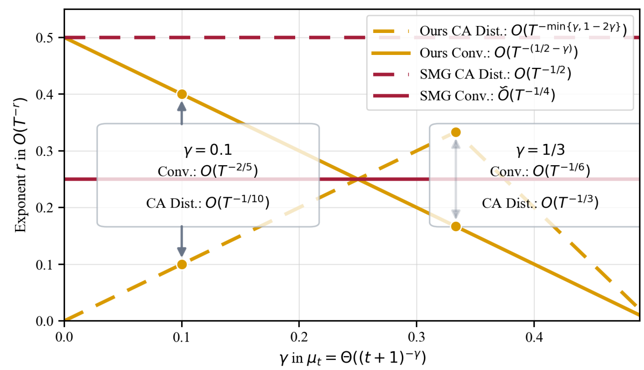

Fig. 2. Rate trade-off under the choice $\mu_t = \Theta((t+1)^{-\gamma})$, $0 < \gamma < 1/2$, with linearly growing mini-batch size $|Z_t| = \Theta(t+1)$ and step size $\alpha = \Theta(T^{-1/2})$. MoRe achieves CA distance exponent $\min\{\gamma, 1-2\gamma\}$ and convergence exponent $1/2 - \gamma$. The additional term $1/(|Z_t|\mu_t^{3/2})$ in Theorem 1 contributes exponent $1 - 3\gamma/2$, which is larger than $1/2 - \gamma$ for the plotted range and therefore is not rate-limiting. The SMG rates are shown as horizontal baselines since they are independent of μ_t.

Beyond convergence in terms of Pareto stationarity, we also analyze how well the stochastic update direction aligns with the corresponding full-batch CA direction. The following theorem bounds the CA direction distance, thereby quantifying the conflict-avoidance behavior of the proposed method.

Theorem 2. *Suppose Assumptions 2 and 4 hold, and let $M = 2$. Let the threshold sequence satisfy $0 < \mu_t \le \bar{\mu}$ for a finite constant $\bar{\mu}$. Then the CA direction distance satisfies*

$$\mathcal{E}_{\mathrm{ca}}(t) = \mathcal{O}\bigg(\frac{1}{|Z_t|\,\mu_t^2} + \frac{1}{|Z_t|} + \mu_t\bigg). \tag{23}$$

In particular, if the mini-batch size grows linearly, i.e., $|Z_t| = \Theta(t+1)$, and $\mu_t = \Theta\Big(\frac{1}{\log(e+t)}\Big)$, then

$$\mathcal{E}_{\mathrm{ca}}(t) = \mathcal{O}\bigg(\frac{1}{\log(e+t)}\bigg). \tag{24}$$

Theorem 2 shows that, in the two-objective case, the CA direction distance is controlled by both the batch size $|Z_t|$ and the regularity threshold μ_t. The logarithmic choice $\mu_t = \Theta(1/\log(e+t))$ matches the schedule used in Theorem 1; it gives a vanishing CA distance while preserving the $\widetilde{\mathcal{O}}(T^{-1/2})$ convergence guarantee. Alternatively, if one prioritizes the CA distance, the choice $\mu_t = \Theta((t+1)^{-1/3})$ yields the sharper rate $\mathcal{E}_{\mathrm{ca}}(t) = \mathcal{O}((t+1)^{-1/3})$. Thus, the choice of μ_t provides a trade-off between conflict-avoidance and convergence speed. The proof of Theorem 2 is deferred to Appendix D.

Figure 2 illustrates the rate trade-off induced by $\mu_t = \Theta((t+1)^{-\gamma})$. Increasing γ improves the CA direction distance up to the optimal choice $\mu_t = \Theta((t+1)^{-1/3})$, but decreases the convergence exponent from $1/2$ to $1/2 - \gamma$, slowing the convergence rate. Thus, μ_t acts as a tuning parameter between conflict-avoidance and convergence speed. In contrast, the SMG rates remain fixed because they are independent of μ_t.

IV. EXPERIMENT

In this section, we empirically evaluate the proposed MoRe method on the Office-Home benchmark, and compare it with several representative MOL baselines.

TABLE II
TEST ACCURACY ON THE OFFICE-HOME DATASET.

Method	Art	Clipart	Product	Real-World	$\Delta_A^{\mathrm{id}}\% \downarrow$
CAGrad [8]	63.75	75.94	89.08	78.27	4.56
MoCo [11]	64.14	79.85	89.62	79.57	2.68
MoDo [2]	65.50	79.44	**89.72**	79.65	2.58
Ours	**66.79**	**80.17**	88.45	**81.84**	**1.21**

A. Experiment setting

We follow the same experimental setting as in [2] and use the LibMTL framework [20]. For each algorithm, we report both individual task performance and a holistic metric $\Delta_A^{\mathrm{id}}\%$, defined as

$$\Delta_A^{\mathrm{id}}\% = \frac{1}{M}\sum_{m=1}^{M}(-1)^{\ell_m}\frac{S_{A,m}-S_{B,m}}{S_{B,m}} \times 100, \tag{25}$$

where M is the number of tasks, $S_{A,m}$ denotes the performance of method A on task m, and $S_{B,m}$ denotes the performance of the corresponding independent single-task learner. Here, $\ell_m = 1$ if a larger value of the metric indicates better performance, and $\ell_m = 0$ otherwise. This metric captures the average performance degradation of an MOL algorithm relative to dedicated single-task learners. Therefore, a smaller $\Delta_A^{\mathrm{id}}\%$ indicates better overall multi-task performance.

B. Office-home benchmark

Next, we evaluate the proposed method on the Office-Home benchmark [21], which is a four-task image classification problem. The four tasks correspond to four visual domains, namely *Art*, *Clipart*, *Product*, and *Real-World*, with 65 object categories in each domain. In our computation of $\Delta_A^{\mathrm{id}}\%$, the independent single-task learner accuracies used as $S_{B,m}$ are 66.86%, 82.02%, 91.38%, and 81.24% for *Art*, *Clipart*, *Product*, and *Real-World*, respectively. These independent baselines are obtained under our experimental setting and may differ from those used in prior works; therefore, the resulting $\Delta_A^{\mathrm{id}}\%$ values may not be numerically identical to reported values in previous works.

As shown in Table II, MoRe improves the performance on Art, Clipart, and Real-World, and achieves a better holistic degradation metric $\Delta_A^{\mathrm{id}}\%$. Although it slightly sacrifices Product accuracy compared with MoDo, the overall results suggest that MoRe provides a favorable trade-off across tasks and is effective for multi-task image classification. Figure 3 shows the convergence behavior of the proposed method. We evaluate the empirical Pareto-stationarity measure $R_S(x_t)$ using full-batch training gradients, matching the quantity analyzed in Theorem 1. Under the parameter setting $\alpha = \Theta(T^{-1/2})$, $|Z_t| = \Theta(t+1)$, and $\mu_t = \Theta(1)$, the stationarity measure decreases steadily, with an empirical trend consistent with the $\mathcal{O}(T^{-1/2})$ rate in Theorem 1.

V. CONCLUSION

This paper studied the continuity property of the MGDA update direction mapping in stochastic MOL and used this property to guide algorithm design. We showed that the CA direction is $1/2$-Hölder continuous on bounded sets, and this exponent is sharp in the worst case. Furthermore, a stronger Lipschitz continuity property holds under a regular or nondegenerate condition. Based on this insight, we proposed MoRe, an adaptive regularity-aware stochastic MGDA method that uses CA direction updates in nondegenerate regimes, where mini-batch perturbations can be controlled, and switches to a fixed scalarization weight in degenerate regimes. By updating in this manner, we showed an improved convergence rate to Pareto stationarity over vanilla stochastic MGDA and a per-iterate CA-direction distance guarantee. Experiments on the Office-Home benchmark further demonstrated the effectiveness of the proposed method in both multi-task performance and convergence behavior. One limitation is that the per-iterate CA-direction distance analysis is restricted to $M = 2$. Extending this analysis to the general multi-objective setting $M > 2$ is left for future work.

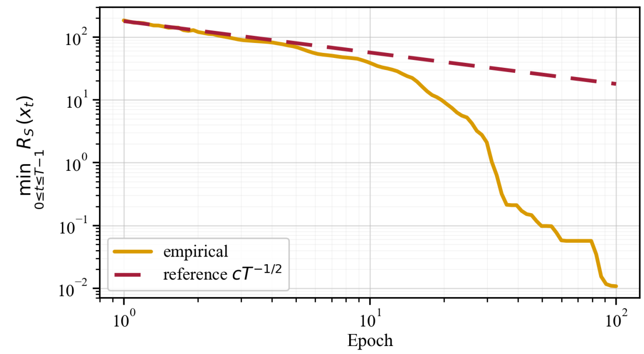

Fig. 3. Convergence curve of the MoRe algorithm on Office-Home. The solid curve shows the empirical Pareto stationarity measure $R_S(x_t)$, while the dashed line shows the reference rate $c/\sqrt{T}$. The observed decay is consistent with the theoretical $\mathcal{O}(T^{-1/2})$ convergence rate established in Theorem 1.

REFERENCES

[1] S. Liu and L. N. Vicente, "The stochastic multi-gradient algorithm for multi-objective optimization and its application to supervised machine learning," *Annals of Operations Research*, vol. 339, no. 3, pp. 1119–1148, 2024.

[2] L. Chen, H. Fernando, Y. Ying, and T. Chen, "Three-way trade-off in multi-objective learning: Optimization, generalization and conflict-avoidance," *Journal of Machine Learning Research*, vol. 25, no. 193, pp. 1–53, 2024.

[3] O. Sener and V. Koltun, "Multi-task learning as multi-objective optimization," in *Advances in Neural Information Processing Systems*, vol. 31, 2018.

[4] F. Ye, B. Lin, Z. Yue, P. Guo, Q. Xiao, and Y. Zhang, "Multi-objective meta learning," in *Advances in Neural Information Processing Systems*, vol. 34, 2021, pp. 21 338–21 351.

[5] L. Chen, S. T. Jose, I. Nikoloska, S. Park, T. Chen, and O. Simeone, "Learning with limited samples: Meta-learning and applications to communication systems," *Foundations and Trends® in Signal Processing*, vol. 17, no. 2, pp. 79–208, 2023.

[6] M. B. Zafar, I. Valera, M. G. Rogriguez, and K. P. Gummadi, "Fairness constraints: Mechanisms for fair classification," in *Proceedings of the 20th International Conference on Artificial Intelligence and Statistics*, ser. Proceedings of Machine Learning Research, vol. 54, 20–22 Apr 2017, pp. 962–970.

[7] H. Mukai, "Algorithms for multicriterion optimization," *IEEE Transactions on Automatic Control*, vol. 25, no. 2, pp. 177–186, 1980.

[8] B. Liu, X. Liu, X. Jin, P. Stone, and Q. Liu, "Conflict-Averse Gradient Descent for Multi-task Learning," in *Proc. Advances Neural Inf. Process. Syst.*, vol. 34, virtual, Dec. 2021, pp. 18 878–18 890.

[9] J. Fliege and B. F. Svaiter, "Steepest descent methods for multicriteria optimization," *Mathematical methods of operations research*, vol. 51, pp. 479–494, 2000.

[10] J.-A. Désidéri, "Multiple-gradient descent algorithm (mgda) for multiobjective optimization," *Comptes Rendus. Mathématique*, vol. 350, no. 5-6, pp. 313–318, 2012.

[11] H. Fernando, H. Shen, M. Liu, S. Chaudhury, K. Murugesan, and T. Chen, "Mitigating gradient bias in multi-objective learning: A provably convergent approach," in *Proc. Int. Conf. Learn. Representations*, Kigali, Rwanda, May 2023.

[12] B. F. Svaiter, "The multiobjective steepest descent direction is not Lipschitz continuous, but is Hölder continuous," *Operations Research Letters*, vol. 46, no. 4, pp. 430–433, 2018.

[13] T. Yu, S. Kumar, A. Gupta, S. Levine, K. Hausman, and C. Finn, "Gradient Surgery for Multi-Task Learning," in *Proc. Advances Neural Inf. Process. Syst.*, vol. 33, virtual, Dec. 2020, pp. 5824–5836.

[14] S. Zhou, W. Zhang, J. Jiang, W. Zhong, J. Gu, and W. Zhu, "On the convergence of stochastic multi-objective gradient manipulation and beyond," in *Advances in Neural Information Processing Systems*, S. Koyejo, S. Mohamed, A. Agarwal, D. Belgrave, K. Cho, and A. Oh, Eds., vol. 35, 2022, pp. 38 103–38 115.

[15] P. Xiao, H. Ban, and K. Ji, "Direction-oriented multi-objective learning: Simple and provable stochastic algorithms," in *Proc. Advances Neural Inf. Process. Syst.*, vol. 36, New Orleans, LA, USA, 2023, pp. 4509–4533.

[16] L. Chen, A. F. M. Saif, Y. Shen, and T. Chen, "FERERO: A flexible framework for preference-guided multi-objective learning," in *Proc. Advances Neural Inf. Process. Syst.*, vol. 37, Vancouver, Canada, 2024, pp. 18 758–18 805.

[17] H. Yang and J. T. Kwok, "Joint gradient balancing for data ordering in finite-sum multi-objective optimization," in *Proc. Int. Conf. Learn. Representations*, Singapore, Apr. 2025.

[18] H. Fernando, L. Chen, S. Lu, P.-Y. Chen, M. Liu, S. Chaudhury, K. Murugesan, G. Liu, M. Wang, and T. Chen, "Variance reduction can improve trade-off in multi-objective learning," in *Proc. IEEE Int. Conf. Acoustics, Speech Signal Process.*, 2024, pp. 6975–6979.

[19] H. Tanabe, E. H. Fukuda, and N. Yamashita, "Proximal gradient methods for multiobjective optimization and their applications," *Computational Optimization and Applications*, vol. 72, no. 2, pp. 339–361, 2019.

[20] B. Lin and Y. Zhang, "LibMTL: A python library for deep multi-task learning," *Journal of Machine Learning Research*, vol. 24, no. 209, pp. 1–7, 2023.

[21] H. Venkateswara, J. Eusebio, S. Chakraborty, and S. Panchanathan, "Deep hashing network for unsupervised domain adaptation," in *Proceedings of the IEEE Conference on Computer Vision and Pattern Recognition*, jul 2017, pp. 5018–5027.

[22] R. A. Horn and C. R. Johnson, *Matrix Analysis*, 2nd ed. Cambridge University Press, 2012.

Appendix

A summary of notation used in this work is listed in Table III for ease of reference.

TABLE III
NOTATION AND DESCRIPTIONS.

Notation	Descriptions
$x \in \mathbb{R}^p$	Model parameter, or decision variable
$z \in \mathcal{Z}$, S, Z	Data point, training sample sequence, and mini-batch, respectively, where $S = (z_1, \dots, z_n) \in \mathcal{Z}^n$, $Z = (\zeta_1, \dots, \zeta_{\lvert Z \rvert})$ is sampled with replacement from S.
$f_{z,m}(x)$, $f_{S,m}(x)$	A scalar-valued objective function evaluated on data point z, with $f_{z,m} : \mathbb{R}^p \to \mathbb{R}$, or on dataset S, $f_{S,m}$, with $f_{S,m}(x) \coloneqq \frac{1}{n} \sum_{i=1}^{n} f_{z_i,m}(x)$
$F_z(x)$, $F_S(x)$, $F_Z(x)$	A vector-valued objective function evaluated on data point z, with $F_z(x) : \mathbb{R}^p \to \mathbb{R}^M$, or on dataset S, with $F_S(x) \coloneqq \frac{1}{n} \sum_{i=1}^{n} F_{z_i}(x)$ or on mini-batch Z, with $F_Z(x) \coloneqq \frac{1}{\lvert Z \rvert} \sum_{r=1}^{\lvert Z \rvert} F_{\zeta_r}(x)$
$\nabla F_S(x)$, $\nabla F_Z(x)$	Gradient matrices of the empirical objective $F_S(x)$ and the mini-batch objective $F_Z(x)$, respectively
$f_m(x)$	A scalar-valued population objective function, $f_m(x) \coloneqq \mathbb{E}_z[f_{z,m}(x)]$
$\nabla f_m(x)$	Gradient of $f_m(x)$, with $\nabla f_m(x) : \mathbb{R}^p \to \mathbb{R}^p$
$F(x)$	A vector-valued population objective, $F(x) \coloneqq \mathbb{E}_z[F_z(x)]$
$\nabla F(x)$	Gradient of $F(x)$, with $\nabla F(x) : \mathbb{R}^p \to \mathbb{R}^{p \times M}$
Q, $q_{Z,m}(x)$	Stochastic gradient matrix and its m-th column, respectively, where $Q = \nabla F_Z(x) = [q_{Z,1}(x), \dots, q_{Z,M}(x)] \in \mathbb{R}^{p \times M}$ $q_{Z,m}(x) = \frac{1}{\lvert Z \rvert} \sum_{r=1}^{\lvert Z \rvert} \nabla f_{\zeta_r,m}(x) \in \mathbb{R}^p$
$\lambda \in \Delta^M$	Weighting parameter in the $(M-1)$-simplex
$\lambda^*(x) \in \Delta^M$	CA weight, optimal solution to (5)
$\lambda_Q^* \in \Delta^M$	Optimal simplex weight for Q, solution to (10)
d_Q, $d(x_t)$, d_t	$d_Q = -Q\lambda_Q^*$ is the CA direction associated with Q, $d(x_t) = -\nabla F_S(x_t)\lambda^*(x_t)$ is the full-batch CA direction at x_t, and $d_t = -Q_t\lambda_t$ is the stochastic update direction used at iteration t.
μ_t	Regularity threshold used by Algorithm 1 to decide whether the stochastic subproblem is nondegenerate.
α_t	Step size for updating the model parameter x

A. *Proof of Lemma 1*

Proof. Throughout this proof, $\|\cdot\|$ denotes the spectral norm for matrices and the Euclidean norm for vectors. By the boundedness condition in Lemma 1 and the inequality $\|Q_i\| \le \|Q_i\|_F$, we have $\|Q_i\| \le B$, $i = 1, 2$. Let $\lambda_{Q_i}^* \in \arg\min_{\lambda \in \Delta^M} \|Q_i\lambda\|^2$, $A_i \coloneqq Q_i^\top Q_i$, $i = 1, 2$. By the reduced nondegeneracy condition in Definition 2, $\mu_{\min}(U^\top Q_i^\top Q_i U) \ge \mu$. Hence, for any $\delta \in \mathbf{1}^\perp$, writing $\delta = Uz$, we have

$$\delta^\top A_i \delta = z^\top U^\top A_i U z \ge \mu \|z\|^2 = \mu \|\delta\|^2. \tag{26}$$

Since any two points in Δ^M differ by a vector in $\mathbf{1}^\perp$, $g_{Q_i}(\lambda) = \|Q_i\lambda\|^2$ is strongly convex on the affine hull of the simplex. Hence $\lambda_{Q_i}^*$ is unique. The optimality conditions give $0 \in 2A_i\lambda_{Q_i}^* + N_{\Delta^M}(\lambda_{Q_i}^*)$, or equivalently,

$$\langle 2A_i\lambda_{Q_i}^*, \lambda - \lambda_{Q_i}^* \rangle \ge 0, \qquad \forall \lambda \in \Delta^M. \tag{27}$$

Let $\delta = \lambda_{Q_1}^* - \lambda_{Q_2}^*$. Taking $\lambda = \lambda_{Q_2}^*$ for $i = 1$ and $\lambda = \lambda_{Q_1}^*$ for $i = 2$ in (27) gives $\langle A_1\lambda_{Q_1}^*, \delta \rangle \le 0$ and $\langle A_2\lambda_{Q_2}^*, \delta \rangle \ge 0$, hence $\langle A_1\lambda_{Q_1}^* - A_2\lambda_{Q_2}^*, \delta \rangle \le 0$. Since $A_1\lambda_{Q_1}^* - A_2\lambda_{Q_2}^* = A_1\delta + (A_1 - A_2)\lambda_{Q_2}^*$, we have $\delta^\top A_1 \delta + \langle (A_1 - A_2)\lambda_{Q_2}^*, \delta \rangle \le 0$. Rearranging this inequality and applying Cauchy–Schwarz gives

$$\delta^\top A_1 \delta \le -\langle (A_1 - A_2)\lambda_{Q_2}^*, \delta \rangle \le \|A_1 - A_2\| \, \|\lambda_{Q_2}^*\| \, \|\delta\|. \tag{28}$$

Because $\lambda_{Q_2}^* \in \Delta^M$, $\|\lambda_{Q_2}^*\| \le 1$. Also, $\delta \in \mathbf{1}^\perp$, so (26) gives $\delta^\top A_1 \delta \ge \mu\|\delta\|^2$. Therefore, combining it with (28) yields

$$\|\delta\| = \|\lambda_{Q_1}^* - \lambda_{Q_2}^*\| \le \frac{1}{\mu} \|A_1 - A_2\|. \tag{29}$$

Moreover, $A_1 - A_2 = Q_1^\top (Q_1 - Q_2) + (Q_1 - Q_2)^\top Q_2$, and hence

$$\|A_1 - A_2\| \le (\|Q_1\| + \|Q_2\|)\|Q_1 - Q_2\| \le 2B\|Q_1 - Q_2\|. \tag{30}$$

Combining (29) and (30), we get

$$\|\lambda_{Q_1}^* - \lambda_{Q_2}^*\| \le \frac{2B}{\mu} \|Q_1 - Q_2\|. \tag{31}$$

Finally, since $d_Q = -Q\lambda_Q^*$, we have $d_{Q_1} - d_{Q_2} = -Q_1(\lambda_{Q_1}^* - \lambda_{Q_2}^*) - (Q_1 - Q_2)\lambda_{Q_2}^*$. Using $\|Q_1\| \le B$, $\|\lambda_{Q_2}^*\| \le 1$, and (31), we obtain

$$\|d_{Q_1} - d_{Q_2}\| \le \|Q_1\|\,\|\lambda_{Q_1}^* - \lambda_{Q_2}^*\| + \|Q_1 - Q_2\|\,\|\lambda_{Q_2}^*\| \le B\|\lambda_{Q_1}^* - \lambda_{Q_2}^*\| + \|Q_1 - Q_2\| \le \left(1 + \frac{2B^2}{\mu}\right)\|Q_1 - Q_2\|. \tag{32}$$

This proves the claim.

□

B. Proof of Lemma 2

Proof. Recall that $d_Q = -Q\lambda_Q^*$, where $\lambda_Q^* \in \arg\min_{\lambda\in\Delta^M}\|Q\lambda\|^2$. Although λ_Q^* may not be unique, the vector $Q\lambda_Q^*$ is unique, since it is the minimum-norm point in the compact convex set $\operatorname{conv}\{q_{Z,1},\cdots,q_{Z,M}\}$. Therefore, d_Q is well-defined. Let $Q, Q' \in \mathbb{R}^{p\times M}$, and let

$$\lambda_Q^* \in \arg\min_{\lambda\in\Delta^M}\|Q\lambda\|^2, \qquad \lambda_{Q'}^* \in \arg\min_{\lambda\in\Delta^M}\|Q'\lambda\|^2. \tag{33}$$

Using the optimality of $Q'\lambda_{Q'}^*$ as the projection of the origin onto $\operatorname{conv}\{q'_{Z,1},\cdots,q'_{Z,M}\}$, we have

$$\left\langle Q'\lambda_{Q'}^*, Q'\lambda_{Q'}^* - Q'\lambda_Q^*\right\rangle \le 0. \tag{34}$$

Expanding the quadratic term and using (34), we obtain

$$\begin{aligned}\|d_Q - d_{Q'}\|^2 = \|Q\lambda_Q^* - Q'\lambda_{Q'}^*\|^2 &= \|Q\lambda_Q^*\|^2 - \|Q'\lambda_{Q'}^*\|^2 + 2\left\langle Q'\lambda_{Q'}^*, Q'\lambda_{Q'}^* - Q\lambda_Q^*\right\rangle \\ &= \|Q\lambda_Q^*\|^2 - \|Q'\lambda_{Q'}^*\|^2 + 2\left\langle Q'\lambda_{Q'}^*, Q'\lambda_{Q'}^* - Q'\lambda_Q^*\right\rangle \\ &\quad + 2\left\langle Q'\lambda_{Q'}^*, Q'\lambda_Q^* - Q\lambda_Q^*\right\rangle \\ &\le \min_{\lambda\in\Delta^M}\|Q\lambda\|^2 - \min_{\lambda\in\Delta^M}\|Q'\lambda\|^2 + 2\|Q'\lambda_{Q'}^*\|\,\|(Q'-Q)\lambda_Q^*\|.\end{aligned} \tag{35}$$

It remains to bound the difference of optimal values. We do so by comparing the two quadratic objectives uniformly over Δ^M

$$\begin{aligned}\min_{\lambda\in\Delta^M}\|Q\lambda\|^2 - \min_{\lambda\in\Delta^M}\|Q'\lambda\|^2 &\le \max_{\lambda\in\Delta^M}\left|\|Q\lambda\|^2 - \|Q'\lambda\|^2\right| \\ &\le \sup_{\lambda\in\Delta^M}\|(Q-Q')\lambda\|\left(\sup_{\lambda\in\Delta^M}\|Q\lambda\| + \sup_{\lambda\in\Delta^M}\|Q'\lambda\|\right).\end{aligned} \tag{36}$$

Combining (35) and (36), and using $\|Q'\lambda_{Q'}^*\| \le \sup_{\lambda\in\Delta^M}\|Q'\lambda\|$, gives

$$\|d_Q - d_{Q'}\|^2 \le 4\max\left\{\sup_{\lambda\in\Delta^M}\|Q\lambda\|, \sup_{\lambda\in\Delta^M}\|Q'\lambda\|\right\}\sup_{\lambda\in\Delta^M}\|(Q-Q')\lambda\|. \tag{37}$$

This is the $1/2$-Hölder bound established in [2]. On the bounded set considered in Lemma 2, Q and Q' satisfy $\|Q\| \le B$ and $\|Q'\| \le B$. Hence,

$$\sup_{\lambda\in\Delta^M}\|Q\lambda\| \le B, \qquad \sup_{\lambda\in\Delta^M}\|Q'\lambda\| \le B, \qquad \sup_{\lambda\in\Delta^M}\|(Q-Q')\lambda\| \le \|Q-Q'\|. \tag{38}$$

Therefore, (37) implies

$$\|d_Q - d_{Q'}\|^2 \le 4B\|Q-Q'\|, \quad \|d_Q - d_{Q'}\| \le 2\sqrt{B}\,\|Q-Q'\|^{1/2}. \tag{39}$$

Hence $Q \mapsto d_Q$ is generally $1/2$-Hölder continuous on any bounded set of gradient matrices. It remains to show that the exponent $1/2$ is sharp. We prove the claim by an explicit counterexample. For $t \in (0, \pi/2)$, define

$$Q_y(t) \coloneqq [q_1^y(t), q_2^y(t)], \qquad Q_z(t) \coloneqq [q_1^z(t), q_2^z(t)], \tag{40}$$

where $q_1^y(t) = (\cos^2 t, \sin t\cos t)$, $q_2^y(t) = (1, 0)$ and $q_1^z(t) = (1, \cos t\sin t)$, $q_2^z(t) = (1, 0)$. We first identify the corresponding CA directions. Observe that

$$q_1^y(t) - q_2^y(t) = (-\sin^2 t, \sin t\cos t). \tag{41}$$

A direct computation gives

$$\begin{aligned}\left(q_1^y(t) - q_2^y(t)\right)^\top q_1^y(t) &= (-\sin^2 t, \sin t\cos t)^\top(\cos^2 t, \sin t\cos t) \\ &= -\sin^2 t\cos^2 t + \sin^2 t\cos^2 t \\ &= 0.\end{aligned} \tag{42}$$

Hence $q_1^y(t) - q_2^y(t)$ is orthogonal to $q_1^y(t)$. Consequently, $q_1^y(t)$ is the projection of the origin onto $\operatorname{conv}\{q_1^y(t), q_2^y(t)\}$, and the CA direction associated with $Q_y(t)$ has the following explicit form.

$$d_{Q_y(t)} = -q_1^y(t) = -(\cos^2 t, \sin t\cos t). \tag{43}$$

Similarly, $q_1^z(t) - q_2^z(t) = (0, \sin t \cos t)$ is orthogonal to $q_2^z(t) = (1, 0)$, and hence $q_2^z(t)$ is the projection of the origin onto $\operatorname{conv}\{q_1^z(t), q_2^z(t)\}$. Thus

$$d_{Q_z(t)} = -q_2^z(t) = -(1, 0). \tag{44}$$

Therefore, the two CA directions differ by

$$\|d_{Q_y(t)} - d_{Q_z(t)}\| = \|q_1^y(t) - q_2^z(t)\| = \|(\sin^2 t, -\sin t \cos t)\| = \sin t. \tag{45}$$

On the other hand, the two matrices differ only in the first coordinate of their first column, since

$$Q_y(t) - Q_z(t) = \begin{bmatrix} -\sin^2 t & 0 \\ 0 & 0 \end{bmatrix}, \qquad \|Q_y(t) - Q_z(t)\| = \sin^2 t. \tag{46}$$

Combining (45) and (46), for any $\eta > \frac{1}{2}$ we have

$$\frac{\|d_{Q_y(t)} - d_{Q_z(t)}\|}{\|Q_y(t) - Q_z(t)\|^\eta} = \frac{\sin t}{(\sin^2 t)^\eta} = (\sin t)^{1-2\eta} \to +\infty \quad \text{as } t \to 0^+. \tag{47}$$

Thus no local Hölder bound with exponent $\eta > \frac{1}{2}$ can hold uniformly for the mapping $Q \mapsto d_Q$. This proves the sharpness of the exponent $\frac{1}{2}$ in the worst case.

We remark that this is consistent with Lemma 1. The Frobenius norms of $Q_y(t)$ and $Q_z(t)$ are uniformly bounded, for instance by $B = 2$. However, for $U = (1, -1)^\top/\sqrt{2}$,

$$\mu_{\min}(U^\top Q_y(t)^\top Q_y(t) U) = \frac{1}{2}\|q_1^y(t) - q_2^y(t)\|^2 = \frac{1}{2}\sin^2 t \to 0 \quad \text{as } t \to 0^+, \tag{48}$$

and the same degeneration holds for $Q_z(t)$. Thus no uniform $\mu > 0$ in Definition 2 covers the family, and the loss of higher-order Hölder regularity occurs exactly where the nondegeneracy condition fails. □

C. Proof of Theorem 1

Proof. Let $\lambda^*(x_t) \in \arg\min_{\lambda \in \Delta^M} \|\nabla F_S(x_t)\lambda\|^2$, so that $\|\nabla F_S(x_t)\lambda^*(x_t)\|^2 = \min_{\lambda \in \Delta^M} \|\nabla F_S(x_t)\lambda\|^2$. Define $H_t := U^\top Q_t^\top Q_t U$, $\bar{H}_t := U^\top \nabla F_S(x_t)^\top \nabla F_S(x_t) U$. We divide the analysis into two cases according to the update rule of Algorithm 1.
Case 1: $\mu_{\min}(U^\top Q_t^\top Q_t U) \geq \mu_t$**.** Then the algorithm uses $\lambda_t \in \arg\min_{\lambda \in \Delta^M} \|Q_t \lambda\|^2$ and updates $x_{t+1} = x_t - \alpha_t Q_t \lambda_t$. The condition $\mu_{\min}(H_t) \geq \mu_t$ gives nondegeneracy for the stochastic gradient matrix Q_t. To compare the stochastic CA direction with the corresponding full-batch direction, we also need the full-batch matrix $\nabla F_S(x_t)$ to be nondegenerate. We therefore define the good perturbation event $\mathcal{G}_t := \big\{\|H_t - \bar{H}_t\| \leq \frac{\mu_t}{2}\big\}$, on which the reduced full-batch curvature is close to its stochastic counterpart. On $\mathcal{G}_t$, since H_t and $\bar{H}_t$ are symmetric matrices, Weyl's inequality [22] gives

$$\mu_{\min}(\bar{H}_t) \geq \mu_{\min}(H_t) - \|H_t - \bar{H}_t\| \geq \mu_t - \frac{\mu_t}{2} = \frac{\mu_t}{2}. \tag{49}$$

Therefore, on this event, both Q_t and $\nabla F_S(x_t)$ satisfy the nondegeneracy condition with curvature lower bound $\frac{1}{2}\mu_t$ required by Lemma 1, which can be used to compare d_{Q_t} and $d_{\nabla F_S(x_t)}$. It remains to control the complement $\mathcal{G}_t^c := \big\{\|H_t - \bar{H}_t\| > \frac{\mu_t}{2}\big\}$. Let $E_t := Q_t - \nabla F_S(x_t)$. Then

$$H_t - \bar{H}_t = U^\top (Q_t^\top Q_t - \nabla F_S(x_t)^\top \nabla F_S(x_t)) U = U^\top \left(Q_t^\top E_t + E_t^\top \nabla F_S(x_t)\right) U. \tag{50}$$

Using $\|U\| = 1$ and the submultiplicativity of the spectral norm, we obtain

$$\|H_t - \bar{H}_t\| \leq \|Q_t^\top E_t + E_t^\top \nabla F_S(x_t)\| \leq \|Q_t^\top E_t\| + \|E_t^\top \nabla F_S(x_t)\| \leq \|Q_t\|\|E_t\| + \|E_t\|\|\nabla F_S(x_t)\| \tag{51}$$

By Assumption 4 and (18), we have $\|Q_t\| \leq \|Q_t\|_F \leq \ell_F$ and $\|\nabla F_S(x_t)\| \leq \|\nabla F_S(x_t)\|_F \leq \ell_F$. Thus ℓ_F directly replaces the bound in all one-step estimates. Thus, combining it with (51), we obtain

$$\|H_t - \bar{H}_t\| \leq 2\ell_F \|Q_t - \nabla F_S(x_t)\| \leq 2\ell_F \|Q_t - \nabla F_S(x_t)\|_F. \tag{52}$$

Conditioning on $\mathcal{F}_t$, Assumption 2 gives $\mathbb{E}\big[\|Q_t - \nabla F_S(x_t)\|_F^2 \mid \mathcal{F}_t\big] \leq \frac{M\sigma^2}{|Z_t|}$. Taking total expectation and using (52),

$$\mathbb{E}\big[\|H_t - \bar{H}_t\|^2\big] \leq \frac{4\ell_F^2 M \sigma^2}{|Z_t|}. \tag{53}$$

By Markov's inequality,

$$\mathbb{P}(\mathcal{G}_t^c) = \mathbb{P}\Big(\|H_t - \bar{H}_t\| > \frac{\mu_t}{2}\Big) \leq \frac{\mathbb{E}[\|H_t - \bar{H}_t\|^2]}{\mu_t^2/4} \leq \frac{16\ell_F^2 M \sigma^2}{|Z_t|\mu_t^2}. \tag{54}$$

By Assumption 3, for any $\lambda \in \Delta^M$, the smoothness of the scalarized empirical objective gives

$$\begin{aligned}\lambda^\top F_S(x_{t+1}) - \lambda^\top F_S(x_t) &\le \langle \nabla F_S(x_t)\lambda, x_{t+1} - x_t\rangle + \frac{\ell_{f,1}}{2}\|x_{t+1} - x_t\|^2 \\ &= -\alpha_t\langle \nabla F_S(x_t)\lambda, Q_t\lambda_t\rangle + \frac{\ell_{f,1}}{2}\alpha_t^2\|Q_t\lambda_t\|^2. \end{aligned} \tag{55}$$

We next bound the inner product term. Write

$$-\langle \nabla F_S(x_t)\lambda, Q_t\lambda_t\rangle = \langle \nabla F_S(x_t)\lambda, \nabla F_S(x_t)\lambda^*(x_t) - Q_t\lambda_t\rangle - \langle \nabla F_S(x_t)\lambda, \nabla F_S(x_t)\lambda^*(x_t)\rangle. \tag{56}$$

Since $\lambda^*(x_t)$ minimizes $\|\nabla F_S(x_t)\lambda\|^2$ over Δ^M, the first-order optimality condition gives

$$\langle \nabla F_S(x_t)\lambda^*(x_t), \nabla F_S(x_t)(\lambda - \lambda^*(x_t))\rangle \ge 0, \tag{57}$$

$$\langle \nabla F_S(x_t)\lambda, \nabla F_S(x_t)\lambda^*(x_t)\rangle \ge \|\nabla F_S(x_t)\lambda^*(x_t)\|^2, \qquad \forall \lambda \in \Delta^M. \tag{58}$$

Moreover, by Assumption 4, $\|\nabla F_S(x_t)\lambda\| \le \ell_f$, for all $\lambda \in \Delta^M$. Combining this with (56) and (58) gives

$$-\langle \nabla F_S(x_t)\lambda, Q_t\lambda_t\rangle \le -\|\nabla F_S(x_t)\lambda^*(x_t)\|^2 + \ell_f\|\nabla F_S(x_t)\lambda^*(x_t) - Q_t\lambda_t\|. \tag{59}$$

Since $\|\nabla F_S(x_t)\lambda^*(x_t) - Q_t\lambda_t\| = \|d_{\nabla F_S(x_t)} - d_{Q_t}\|$, we now bound the direction difference separately on $\mathcal{G}_t$ and $\mathcal{G}_t^c$. On $\mathcal{G}_t$, by (49), Lemma 1 applies to Q_t and $\nabla F_S(x_t)$. Hence,

$$\|d_{Q_t} - d_{\nabla F_S(x_t)}\| \le \ell_{d,t}\|Q_t - \nabla F_S(x_t)\|_F, \qquad \ell_{d,t} = 1 + \frac{4\ell_F^2}{\mu_t}. \tag{60}$$

Here Lemma 1 is applied with nondegeneracy constant $\mu_t/2$, and the Frobenius norm is used through $\|A\| \le \|A\|_F$. On $\mathcal{G}_t^c$, we use the $1/2$-Hölder continuity from Lemma 2. Since Assumption 4 gives $\|Q_t\|_F \le \ell_F$ and $\|\nabla F_S(x_t)\|_F \le \ell_F$, both Q_t and $\nabla F_S(x_t)$ are bounded by ℓ_F. Thus,

$$\|d_{Q_t} - d_{\nabla F_S(x_t)}\| \le 2\sqrt{\ell_F}\,\|Q_t - \nabla F_S(x_t)\|_F^{1/2}. \tag{61}$$

Combining (60) and (61), on the regular branch we first obtain the pathwise case-by-case bound

$$\|d_{Q_t} - d_{\nabla F_S(x_t)}\| \le \ell_{d,t}\|Q_t - \nabla F_S(x_t)\|_F\,\mathbf{1}_{\mathcal{G}_t} + 2\sqrt{\ell_F}\,\|Q_t - \nabla F_S(x_t)\|_F^{1/2}\,\mathbf{1}_{\mathcal{G}_t^c}, \tag{62}$$

where the first term follows from (60) on $\mathcal{G}_t$ and the second from (61) on $\mathcal{G}_t^c$. Since both terms are nonnegative, dropping $\mathbf{1}_{\mathcal{G}_t}$ only weakens the bound and yields

$$\|d_{Q_t} - d_{\nabla F_S(x_t)}\| \le \ell_{d,t}\|Q_t - \nabla F_S(x_t)\|_F + 2\sqrt{\ell_F}\,\|Q_t - \nabla F_S(x_t)\|_F^{1/2}\mathbf{1}_{\mathcal{G}_t^c}. \tag{63}$$

Substituting (63) into (59), and then into (55), gives

$$\begin{aligned}\alpha_t\|\nabla F_S(x_t)\lambda^*(x_t)\|^2 \le{}& \lambda^\top F_S(x_t) - \lambda^\top F_S(x_{t+1}) + \alpha_t\ell_f\ell_{d,t}\|Q_t - \nabla F_S(x_t)\|_F \\ &+ 2\alpha_t\ell_f\sqrt{\ell_F}\,\|Q_t - \nabla F_S(x_t)\|_F^{1/2}\mathbf{1}_{\mathcal{G}_t^c} + \frac{\ell_{f,1}}{2}\alpha_t^2\|Q_t\lambda_t\|^2. \end{aligned} \tag{64}$$

Using Assumption 4 and $\lambda_t \in \Delta^M$, we have $\|Q_t\lambda_t\| \le \ell_f \le \ell_F$. Thus, taking $\lambda = \lambda_0$, we obtain

$$\begin{aligned}\alpha_t\|\nabla F_S(x_t)\lambda^*(x_t)\|^2 \le{}& \lambda_0^\top F_S(x_t) - \lambda_0^\top F_S(x_{t+1}) + \alpha_t\ell_f\ell_{d,t}\|Q_t - \nabla F_S(x_t)\|_F \\ &+ 2\alpha_t\ell_f\sqrt{\ell_F}\,\|Q_t - \nabla F_S(x_t)\|_F^{1/2}\mathbf{1}_{\mathcal{G}_t^c} + \frac{\ell_{f,1}}{2}\alpha_t^2\ell_F^2. \end{aligned} \tag{65}$$

Case 2: $\mu_{\min}(U^\top Q_t^\top Q_t U) < \mu_t$. In this case, the algorithm sets $\lambda_t = \lambda_0$, where $\lambda_0 \in \Delta^M$ is fixed. Plugging $x_{t+1} = x_t - \alpha_t Q_t\lambda_0$ into Assumption 3 with $\lambda = \lambda_0$, we obtain

$$\begin{aligned}\lambda_0^\top F_S(x_{t+1}) - \lambda_0^\top F_S(x_t) &\le -\alpha_t\langle \nabla F_S(x_t)\lambda_0, Q_t\lambda_0\rangle + \frac{\ell_{f,1}}{2}\alpha_t^2\|Q_t\lambda_0\|^2 \\ &\le -\alpha_t\langle \nabla F_S(x_t)\lambda_0, Q_t\lambda_0\rangle + \frac{\ell_{f,1}}{2}\alpha_t^2\ell_F^2. \end{aligned} \tag{66}$$

We use the pathwise decomposition

$$\langle \nabla F_S(x_t)\lambda_0, Q_t\lambda_0\rangle = \|\nabla F_S(x_t)\lambda_0\|^2 + \langle \nabla F_S(x_t)\lambda_0, (Q_t - \nabla F_S(x_t))\lambda_0\rangle. \tag{67}$$

Applying the Cauchy–Schwarz inequality to the second term of (67), together with $\|\nabla F_S(x_t)\lambda_0\| \le \ell_f$ and $\|(Q_t - \nabla F_S(x_t))\lambda_0\| \le \|Q_t - \nabla F_S(x_t)\|_F$, we obtain

$$\begin{aligned}\langle \nabla F_S(x_t)\lambda_0, Q_t\lambda_0\rangle &\ge \|\nabla F_S(x_t)\lambda_0\|^2 - \|\nabla F_S(x_t)\lambda_0\|\,\|(Q_t - \nabla F_S(x_t))\lambda_0\| \\ &\ge \|\nabla F_S(x_t)\lambda_0\|^2 - \ell_f\|Q_t - \nabla F_S(x_t)\|_F. \end{aligned} \tag{68}$$

Since $\lambda^*(x_t)$ minimizes $\|\nabla F_S(x_t)\lambda\|^2$ over Δ^M, $\|\nabla F_S(x_t)\lambda^*(x_t)\|^2 \le \|\nabla F_S(x_t)\lambda_0\|^2$. Therefore,

$$\langle \nabla F_S(x_t)\lambda_0, Q_t\lambda_0\rangle \ge \|\nabla F_S(x_t)\lambda^*(x_t)\|^2 - \ell_f\|Q_t - \nabla F_S(x_t)\|_F. \tag{69}$$

Substituting this into (66) and rearranging gives

$$\alpha_t\|\nabla F_S(x_t)\lambda^*(x_t)\|^2 \le \lambda_0^\top F_S(x_t) - \lambda_0^\top F_S(x_{t+1}) + \alpha_t\ell_f\|Q_t - \nabla F_S(x_t)\|_F + \frac{\ell_{f,1}}{2}\alpha_t^2\ell_F^2. \tag{70}$$

Unified bound for both cases. Since $\ell_{d,t} \ge 1$, both (65) and (70) imply the following pathwise bound:

$$\begin{aligned}\alpha_t\|\nabla F_S(x_t)\lambda^*(x_t)\|^2 \le{}& \lambda_0^\top F_S(x_t) - \lambda_0^\top F_S(x_{t+1}) + \alpha_t\ell_f\ell_{d,t}\|Q_t - \nabla F_S(x_t)\|_F \\ &+ 2\alpha_t\ell_f\sqrt{\ell_F}\,\|Q_t - \nabla F_S(x_t)\|_F^{1/2}\mathbf{1}_{\mathcal{G}_t^c} + \frac{\ell_{f,1}}{2}\alpha_t^2\ell_F^2.\end{aligned} \tag{71}$$

Taking expectation in (71), we get

$$\begin{aligned}\alpha_t\mathbb{E}[\|\nabla F_S(x_t)\lambda^*(x_t)\|^2] \le{}& \mathbb{E}\big[\lambda_0^\top F_S(x_t) - \lambda_0^\top F_S(x_{t+1})\big] + \alpha_t\ell_f\ell_{d,t}\mathbb{E}[\|Q_t - \nabla F_S(x_t)\|_F] \\ &+ 2\alpha_t\ell_f\sqrt{\ell_F}\,\mathbb{E}\Big[\|Q_t - \nabla F_S(x_t)\|_F^{1/2}\mathbf{1}_{\mathcal{G}_t^c}\Big] + \frac{\ell_{f,1}}{2}\alpha_t^2\ell_F^2.\end{aligned} \tag{72}$$

Conditioning on $\mathcal{F}_t$, Assumption 2 gives

$$\mathbb{E}\big[\|Q_t - \nabla F_S(x_t)\|_F^2 \mid \mathcal{F}_t\big] = \sum_{m=1}^{M}\mathbb{E}\big[\|q_{Z_t,m}(x_t) - \nabla f_{S,m}(x_t)\|^2 \mid \mathcal{F}_t\big] \le \frac{M\sigma^2}{|Z_t|}. \tag{73}$$

Therefore, by Jensen's inequality,

$$\mathbb{E}[\|Q_t - \nabla F_S(x_t)\|_F \mid \mathcal{F}_t] \le \frac{\sqrt{M}\sigma}{\sqrt{|Z_t|}}. \tag{74}$$

Taking total expectations and using the tower property yield

$$\mathbb{E}\big[\|Q_t - \nabla F_S(x_t)\|_F^2\big] \le \frac{M\sigma^2}{|Z_t|}, \tag{75}$$

$$\mathbb{E}[\|Q_t - \nabla F_S(x_t)\|_F] \le \frac{\sqrt{M}\sigma}{\sqrt{|Z_t|}}. \tag{76}$$

It remains to bound the bad-event term. By Hölder's inequality with conjugate exponents 4 and $4/3$, we have

$$\mathbb{E}\Big[\|Q_t - \nabla F_S(x_t)\|_F^{1/2}\mathbf{1}_{\mathcal{G}_t^c}\Big] \le \big(\mathbb{E}[\|Q_t - \nabla F_S(x_t)\|_F^2]\big)^{1/4}\left(\mathbb{P}(\mathcal{G}_t^c)\right)^{3/4}. \tag{77}$$

Using (75) and (54), we obtain

$$\mathbb{E}\Big[\|Q_t - \nabla F_S(x_t)\|_F^{1/2}\mathbf{1}_{\mathcal{G}_t^c}\Big] \le \left(\frac{M\sigma^2}{|Z_t|}\right)^{1/4}\left(\frac{16\ell_F^2M\sigma^2}{|Z_t|\mu_t^2}\right)^{3/4} = \mathcal{O}\!\left(\frac{1}{|Z_t|\mu_t^{3/2}}\right). \tag{78}$$

Substituting (76) and (78) into (72), and using that $\ell_{d,t} = 1 + 4\ell_F^2/\mu_t$ with $0 < \mu_t \le \bar{\mu}$, we obtain

$$\alpha_t\mathbb{E}[\|\nabla F_S(x_t)\lambda^*(x_t)\|^2] \le \mathbb{E}\big[\lambda_0^\top F_S(x_t) - \lambda_0^\top F_S(x_{t+1})\big] \quad + \alpha_t\mathcal{O}\!\left(\frac{1}{\sqrt{|Z_t|}} + \frac{1}{\mu_t\sqrt{|Z_t|}} + \frac{1}{|Z_t|\mu_t^{3/2}}\right) + \mathcal{O}(\alpha_t^2). \tag{79}$$

Summing (79) over $t = 0, \ldots, T-1$, dividing both sides by αT, and setting $\alpha_t = \alpha$ for all t, we obtain

$$\begin{aligned}\frac{1}{T}\sum_{t=0}^{T-1}\mathbb{E}[\|\nabla F_S(x_t)\lambda^*(x_t)\|^2] \le{}& \frac{\mathbb{E}\big[\lambda_0^\top F_S(x_0) - \lambda_0^\top F_S(x_T)\big]}{\alpha T} \\ &+ \mathcal{O}\!\left(\frac{1}{T}\sum_{t=0}^{T-1}\frac{1}{\sqrt{|Z_t|}} + \frac{1}{T}\sum_{t=0}^{T-1}\frac{1}{\mu_t\sqrt{|Z_t|}} + \frac{1}{T}\sum_{t=0}^{T-1}\frac{1}{|Z_t|\mu_t^{3/2}}\right) + \mathcal{O}(\alpha).\end{aligned} \tag{80}$$

By the definition of $\lambda^*(x_t)$,

$$\mathbb{E}\left[\min_{0\le t\le T-1} R_S(x_t)\right] = \mathbb{E}\left[\min_{0\le t\le T-1}\|\nabla F_S(x_t)\lambda^*(x_t)\|^2\right] \le \frac{1}{T}\sum_{t=0}^{T-1}\mathbb{E}\big[\|\nabla F_S(x_t)\lambda^*(x_t)\|^2\big]. \tag{81}$$

By Assumption 1 and $\lambda_0 \in \Delta^M$, the scalarized objective $\lambda_0^\top F_S(\cdot)$ is bounded below. Hence, there exists a finite constant Δ_F such that $\mathbb{E}\big[\lambda_0^\top F_S(x_0) - \lambda_0^\top F_S(x_T)\big] \le \Delta_F < \infty$. Therefore, $\frac{\mathbb{E}\big[\lambda_0^\top F_S(x_0) - \lambda_0^\top F_S(x_T)\big]}{\alpha T} \le \mathcal{O}\big(\frac{1}{\alpha T}\big)$. Thus, combining (81) with (80) proves the desired averaged stationarity bound:

$$\mathbb{E}\left[\min_{0\le t\le T-1} R_S(x_t)\right] \le \mathcal{O}\left(\frac{1}{\alpha T} + \alpha + \frac{1}{T}\sum_{t=0}^{T-1}\frac{1}{\sqrt{|Z_t|}} + \frac{1}{T}\sum_{t=0}^{T-1}\frac{1}{\mu_t\sqrt{|Z_t|}} + \frac{1}{T}\sum_{t=0}^{T-1}\frac{1}{|Z_t|\mu_t^{3/2}}\right). \tag{82}$$

If $\mu_t = \Theta(1)$, then there exists a constant $\underline{\mu} > 0$ such that $\mu_t \ge \underline{\mu}$ for all t. Hence, $\frac{1}{T}\sum_{t=0}^{T-1}\frac{1}{\mu_t\sqrt{|Z_t|}} \le \frac{1}{\underline{\mu}T}\sum_{t=0}^{T-1}\frac{1}{\sqrt{|Z_t|}}$, and $\frac{1}{T}\sum_{t=0}^{T-1}\frac{1}{|Z_t|\mu_t^{3/2}} \le \frac{1}{\underline{\mu}^{3/2}T}\sum_{t=0}^{T-1}\frac{1}{|Z_t|}$. Since $|Z_t| = \Theta(t+1)$, we have $T^{-1}\sum_{t=0}^{T-1}|Z_t|^{-1/2} = \mathcal{O}(T^{-1/2})$ and $T^{-1}\sum_{t=0}^{T-1}|Z_t|^{-1} = \mathcal{O}(\log T/T) = \mathcal{O}(T^{-1/2})$. Choosing $\alpha = \Theta(T^{-1/2})$ and $|Z_t| = \Theta(t+1)$ gives $\mathbb{E}[\min_{0\le t\le T-1} R_S(x_t)] = \mathcal{O}(T^{-1/2})$. Moreover, when the threshold decays logarithmically as $\mu_t = \Theta\left(\frac{1}{\log(e+t)}\right)$, under $|Z_t| = \Theta(t+1)$ and $\alpha = \Theta(T^{-1/2})$, the rate is $\widetilde{\mathcal{O}}(T^{-1/2})$.

□

D. Proof of Theorem 2

Proof. Since $M = 2$, write $\nabla F_S(x_t) = [\nabla f_{S,1}(x_t), \nabla f_{S,2}(x_t)]$ and $Q_t = [q_{Z_t,1}(x_t), q_{Z_t,2}(x_t)]$. For brevity in this proof, write $q_{Z_t,m} = q_{Z_t,m}(x_t)$ for $m = 1, 2$. Let $d(x_t) = -\nabla F_S(x_t)\lambda^*(x_t)$, where $\lambda^*(x_t) \in \arg\min_{\lambda\in\Delta^2}\|\nabla F_S(x_t)\lambda\|^2$, and let $d_t = -Q_t\lambda_t$. By Assumption 4 and (18), $\|Q_t\|_F \le \ell_F$ and $\|\nabla F_S(x_t)\|_F \le \ell_F$, so the bad-event estimate (54) applies directly with ℓ_F. Define the regular branch event $\mathcal{R}_t := \big\{\mu_{\min}(U^\top Q_t^\top Q_t U) \ge \mu_t\big\}$. Then $\mathcal{R}_t^c = \big\{\mu_{\min}(U^\top Q_t^\top Q_t U) < \mu_t\big\}$. By the definition of $\mathcal{E}_{\rm ca}(t)$ and Jensen's inequality,

$$\mathcal{E}_{\rm ca}(t) = \|\mathbb{E}[d_t - d(x_t)]\|^2 = \|\mathbb{E}[\mathbb{E}[d_t - d(x_t) \mid \mathcal{F}_t]]\|^2 \le \mathbb{E}\Big[\|\mathbb{E}[d_t - d(x_t) \mid \mathcal{F}_t]\|^2\Big] \le \mathbb{E}\big[\|d_t - d(x_t)\|^2\big]. \tag{83}$$

We split the right-hand side according to the two branches of Algorithm 1:

$$\mathbb{E}\big[\|d_t - d(x_t)\|^2\big] = \mathbb{E}\big[\mathbf{1}_{\mathcal{R}_t}\|d_t - d(x_t)\|^2\big] + \mathbb{E}\big[\mathbf{1}_{\mathcal{R}_t^c}\|d_t - d(x_t)\|^2\big]. \tag{84}$$

The two terms are controlled by different mechanisms. On the regular branch $\mathcal{R}_t$, the stochastic MGDA subproblem is sufficiently nondegenerate, so the direction perturbation can be bounded by the Lipschitz continuity of the CA direction, up to the bad-event correction already used in the proof of Theorem 1. On the degenerate branch $\mathcal{R}_t^c$, we do not rely on Lipschitz continuity. Instead, when $M = 2$, small tangent curvature directly implies $\|q_{Z_t,1} - q_{Z_t,2}\|^2 = O(\mu_t)$, which controls the discrepancy between the fallback direction and the full-batch CA direction. We next bound the regular and degenerate branch terms separately.

Case 1: If $\mu_{\min}(U^\top Q_t^\top Q_t U) \ge \mu_t$, using the regular-branch direction perturbation bound (63) from the proof of Theorem 1, we have

$$\|d_t - d(x_t)\| \le \ell_{d,t}\|Q_t - \nabla F_S(x_t)\|_F + 2\sqrt{\ell_F}\,\|Q_t - \nabla F_S(x_t)\|_F^{1/2}\mathbf{1}_{\mathcal{G}_t^c}, \tag{85}$$

where $\mathcal{G}_t^c = \big\{\|U^\top Q_t^\top Q_t U - U^\top \nabla F_S(x_t)^\top \nabla F_S(x_t) U\|_2 > \frac{\mu_t}{2}\big\}$. Squaring (85) and using $(a+b)^2 \le 2a^2 + 2b^2$, we obtain

$$\|d_t - d(x_t)\|^2 \le 2\ell_{d,t}^2\|Q_t - \nabla F_S(x_t)\|_F^2 + 8\ell_F\|Q_t - \nabla F_S(x_t)\|_F\mathbf{1}_{\mathcal{G}_t^c}. \tag{86}$$

By conditioning on $\mathcal{F}_t$, using Assumption 2, and then taking total expectation, since $M = 2$, $\mathbb{E}\big[\|Q_t - \nabla F_S(x_t)\|_F^2\big] \le \frac{2\sigma^2}{|Z_t|}$. Moreover, by the Cauchy–Schwarz inequality and the bad-event probability bound (54) from the proof of Theorem 1,

$$\mathbb{E}\big[\|Q_t - \nabla F_S(x_t)\|_F\mathbf{1}_{\mathcal{G}_t^c}\big] \le \big(\mathbb{E}\big[\|Q_t - \nabla F_S(x_t)\|_F^2\big]\big)^{1/2}(\mathbb{P}(\mathcal{G}_t^c))^{1/2} \le \left(\frac{2\sigma^2}{|Z_t|}\right)^{1/2}\left(\frac{32\ell_F^2\sigma^2}{|Z_t|\mu_t^2}\right)^{1/2} = \mathcal{O}\left(\frac{1}{|Z_t|\mu_t}\right). \tag{87}$$

Using $\ell_{d,t} = 1 + 4\ell_F^2/\mu_t$, $\mathbb{E}\big[\|Q_t - \nabla F_S(x_t)\|_F^2\big] \le \frac{2\sigma^2}{|Z_t|}$, and (87) in (86), we obtain

$$\mathbb{E}\big[\mathbf{1}_{\mathcal{R}_t}\|d_t - d(x_t)\|^2\big] = \mathcal{O}\left(\frac{1}{|Z_t|\mu_t^2}\right), \tag{88}$$

where the term $\mathcal{O}(1/(|Z_t|\mu_t))$ is absorbed into $\mathcal{O}(1/(|Z_t|\mu_t^2))$ since $0 < \mu_t \le \bar{\mu}$.

Case 2: If $\mu_{\min}(U^\top Q_t^\top Q_t U) < \mu_t$, every $\lambda \in \Delta^2$ can be written as $\lambda = (a, 1-a)$ for some $a \in [0,1]$. Write

$$\lambda_t = (\hat{a}_t, 1 - \hat{a}_t), \qquad \lambda^*(x_t) = (a_t^*, 1 - a_t^*), \tag{89}$$

with $a_t^*, \hat{a}_t \in [0,1]$. Then

$$d_t = -(\hat{a}_t q_{Z_t,1} + (1-\hat{a}_t)q_{Z_t,2}), \qquad d(x_t) = -(a_t^*\nabla f_{S,1}(x_t) + (1-a_t^*)\nabla f_{S,2}(x_t)). \tag{90}$$

Adding and subtracting $a_t^* q_{Z_t,1} + (1-a_t^*) q_{Z_t,2}$, we obtain

$$d_t - d(x_t) = (a_t^* - \hat{a}_t)(q_{Z_t,1} - q_{Z_t,2}) + a_t^*(\nabla f_{S,1}(x_t) - q_{Z_t,1}) + (1-a_t^*)(\nabla f_{S,2}(x_t) - q_{Z_t,2}). \tag{91}$$

Thus, using $a_t^*, \hat{a}_t \in [0,1]$,

$$\begin{aligned}\|d_t - d(x_t)\| &\le |a_t^* - \hat{a}_t| \, \|q_{Z_t,1} - q_{Z_t,2}\| + a_t^* \|\nabla f_{S,1}(x_t) - q_{Z_t,1}\| + (1-a_t^*)\|\nabla f_{S,2}(x_t) - q_{Z_t,2}\| \\ &\le \|q_{Z_t,1} - q_{Z_t,2}\| + \|\nabla f_{S,1}(x_t) - q_{Z_t,1}\| + \|\nabla f_{S,2}(x_t) - q_{Z_t,2}\|. \end{aligned} \tag{92}$$

Squaring both sides and using $\|u+v+w\|^2 \le 3\|u\|^2 + 3\|v\|^2 + 3\|w\|^2$, we get

$$\|d_t - d(x_t)\|^2 \le 3\|q_{Z_t,1} - \nabla f_{S,1}(x_t)\|^2 + 3\|q_{Z_t,2} - \nabla f_{S,2}(x_t)\|^2 + 3\|q_{Z_t,1} - q_{Z_t,2}\|^2. \tag{93}$$

For $M=2$, the tangent space of the simplex is $\operatorname{span}\{(1,-1)^\top\}$. The reduced curvature matrix $U^\top Q_t^\top Q_t U$ is a scalar, and

$$\mu_{\min}(U^\top Q_t^\top Q_t U) = \frac{1}{2}(q_{Z_t,1} - q_{Z_t,2})^\top (q_{Z_t,1} - q_{Z_t,2}) = \frac{1}{2}\|q_{Z_t,1} - q_{Z_t,2}\|^2. \tag{94}$$

Equivalently, for $v = (1,-1)^\top$, we have $Q_t v = q_{Z_t,1} - q_{Z_t,2}$, and $U = v/\sqrt{2}$. Therefore, under the case condition $\mu_{\min}(U^\top Q_t^\top Q_t U) < \mu_t$, we have $\|q_{Z_t,1} - q_{Z_t,2}\|^2 < 2\mu_t$. Multiplying (93) by $\mathbf{1}_{\mathcal{R}_t^c}$, bounding the last term via $\mathbf{1}_{\mathcal{R}_t^c}\|q_{Z_t,1} - q_{Z_t,2}\|^2 < 2\mu_t$, dropping the indicator on the two variance terms, and taking expectations yields

$$\mathbb{E}\big[\mathbf{1}_{\mathcal{R}_t^c}\|d_t - d(x_t)\|^2\big] \le 3\mathbb{E}\big[\|q_{Z_t,1} - \nabla f_{S,1}(x_t)\|^2\big] + 3\mathbb{E}\big[\|q_{Z_t,2} - \nabla f_{S,2}(x_t)\|^2\big] + 6\mu_t. \tag{95}$$

By Assumption 2, for $m=1,2$, $\mathbb{E}\big[\|q_{Z_t,m} - \nabla f_{S,m}(x_t)\|^2\big] \le \frac{\sigma^2}{|Z_t|}$. Combining this fact and (95), we obtain

$$\mathbb{E}\big[\mathbf{1}_{\mathcal{R}_t^c}\|d_t - d(x_t)\|^2\big] \le \frac{6\sigma^2}{|Z_t|} + 6\mu_t. \tag{96}$$

Unified bound for both cases. Combining these two cases, from (88) and (96), we conclude that

$$\mathcal{E}_{\mathrm{ca}}(t) = \mathcal{O}\left(\frac{1}{|Z_t|\,\mu_t^2} + \frac{1}{|Z_t|} + \mu_t\right). \tag{97}$$

For the schedule used in Theorem 1, i.e., $|Z_t| = \Theta(t+1)$ and $\mu_t = \Theta\Big(\frac{1}{\log(e+t)}\Big)$, we obtain

$$\mathcal{E}_{\mathrm{ca}}(t) = \mathcal{O}\left(\frac{1}{\log(e+t)}\right). \tag{98}$$

This proves the theorem. $\square$